

Electronic Supplementary Information

Equipping carbon dots in a defect-containing MOF *via* self-carbonization for explosive sensing

Ling-Xiao Li,^{‡a} Shan He,^{‡a} Shanshan Zeng,^b Wan-Tao Chen,^c Jia-Wen Ye,^{*c} Hao-Long Zhou^{*a, d} and Xiao-Chun Huang^{a, e}

^a *Department of Chemistry and Key Laboratory for Preparation and Application of Ordered Structural Materials of Guangdong Province, Shantou University, Shantou 515063, China.*

^b *Central Laboratory, Shantou University, Shantou 515063, China.*

^c *School of Biotechnology and Health Science, Wuyi University, Jiangmen 529000, P. R. China.*

^d *Key Laboratory of Organosilicon Chemistry and Material Technology of Ministry of Education, Hangzhou Normal University, Hangzhou 311121, P. R. China.*

^e *Chemistry and Chemical Engineering Guangdong Laboratory, Shantou 515031, China.*

[‡] These authors contributed equally to this work.

^{*} Corresponding authors.

E-mail: wychemyjw@126.com; hlzhou@stu.edu.cn

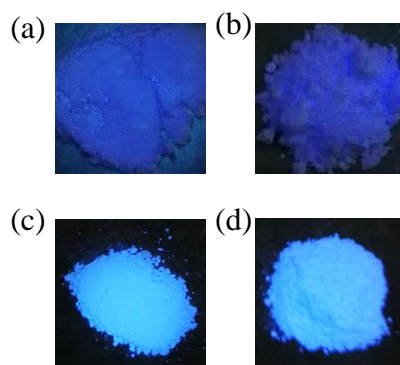


Figure S1. Photographs of (a) UiO-66, (b) DUiO-66, (c) UiO-66N and (d) DUiO-66N under 365-nm UV light. UiO-66 and DUiO-66 (*i.e.* defect-containing UiO-66) were according to the literature procedure.^[1]

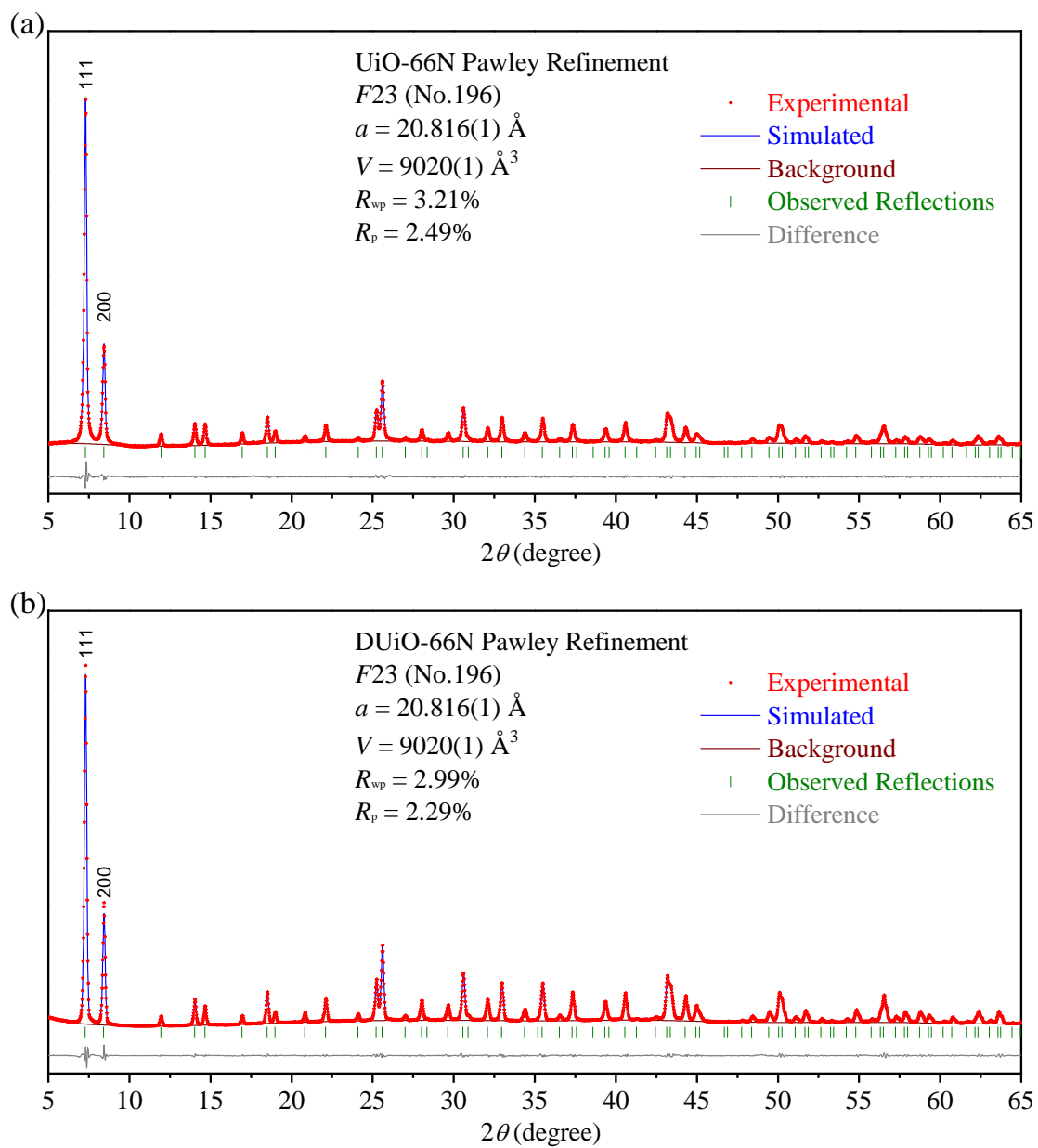


Figure S2. PXRD refinement of (a) UiO-66N and (b) DUiO-66N.

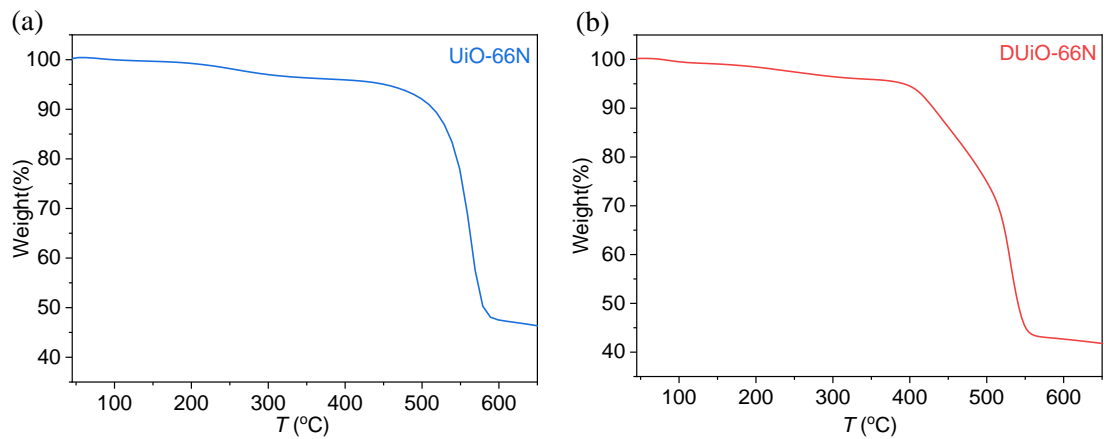


Figure S3. TGA curves of (a) UiO-66N and (b) DUiO-66N under nitrogen.

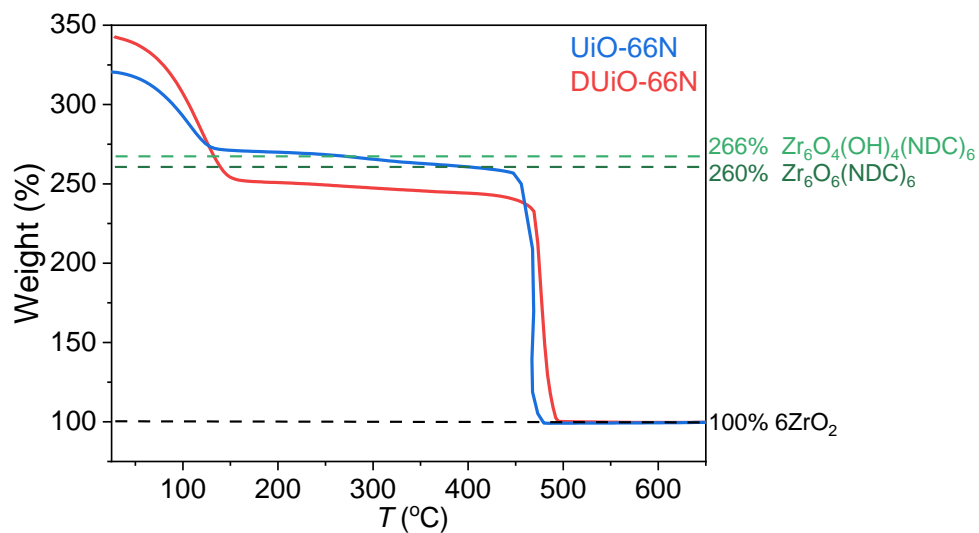


Figure S4. TGA curves of UiO-66N and DUiO-66N under oxygen.

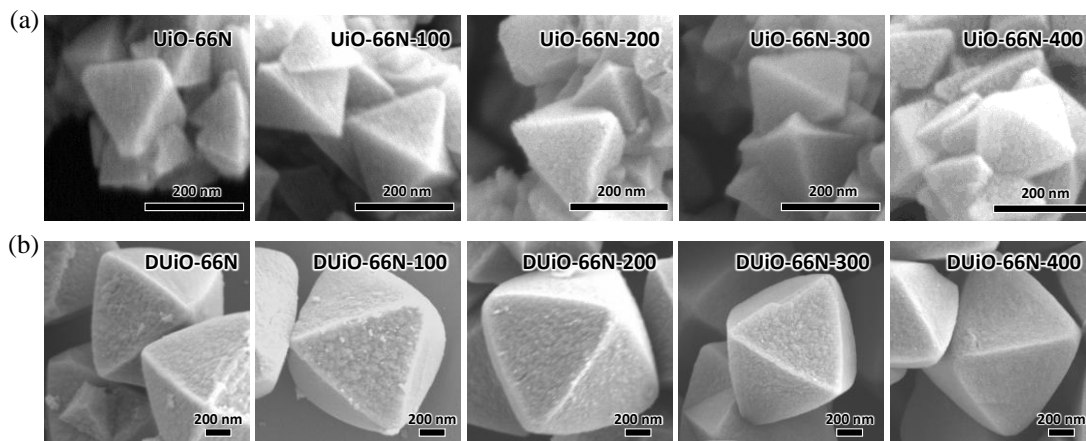


Figure S5. SEM images of (a) UiO-66N and (b) DUiO-66N.

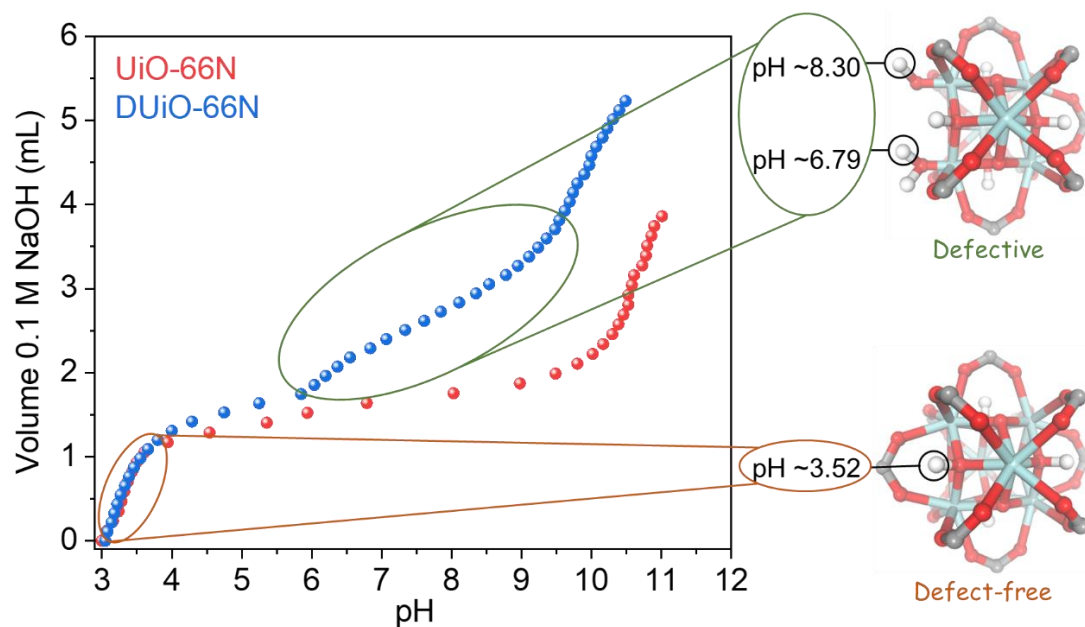


Figure S6. Potentiometric acid–base titration plots of UiO-66N and DUiO-66N.

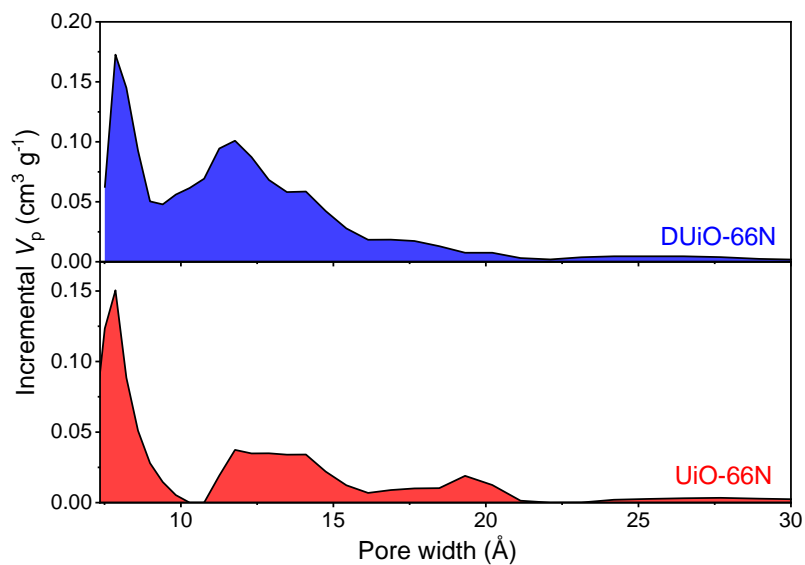


Figure S7. Pore size distribution of UiO-66N and DUiO-66N, derived from the non-local density functional theory (NLDFT) analysis of standard N₂ adsorption isotherms measured at 77 K.

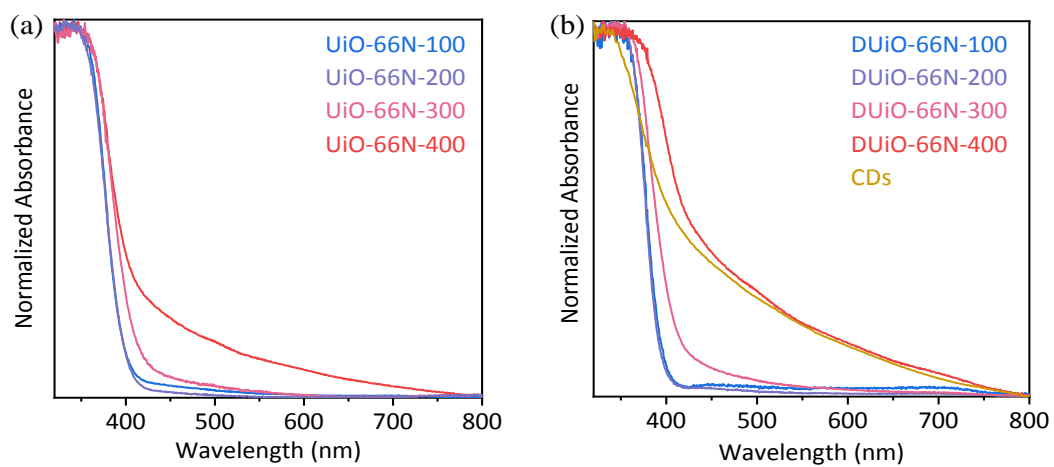


Figure S8. UV-vis absorption spectra of (a) UiO-66N-X, (b) DUiO-66N-X and CDs.

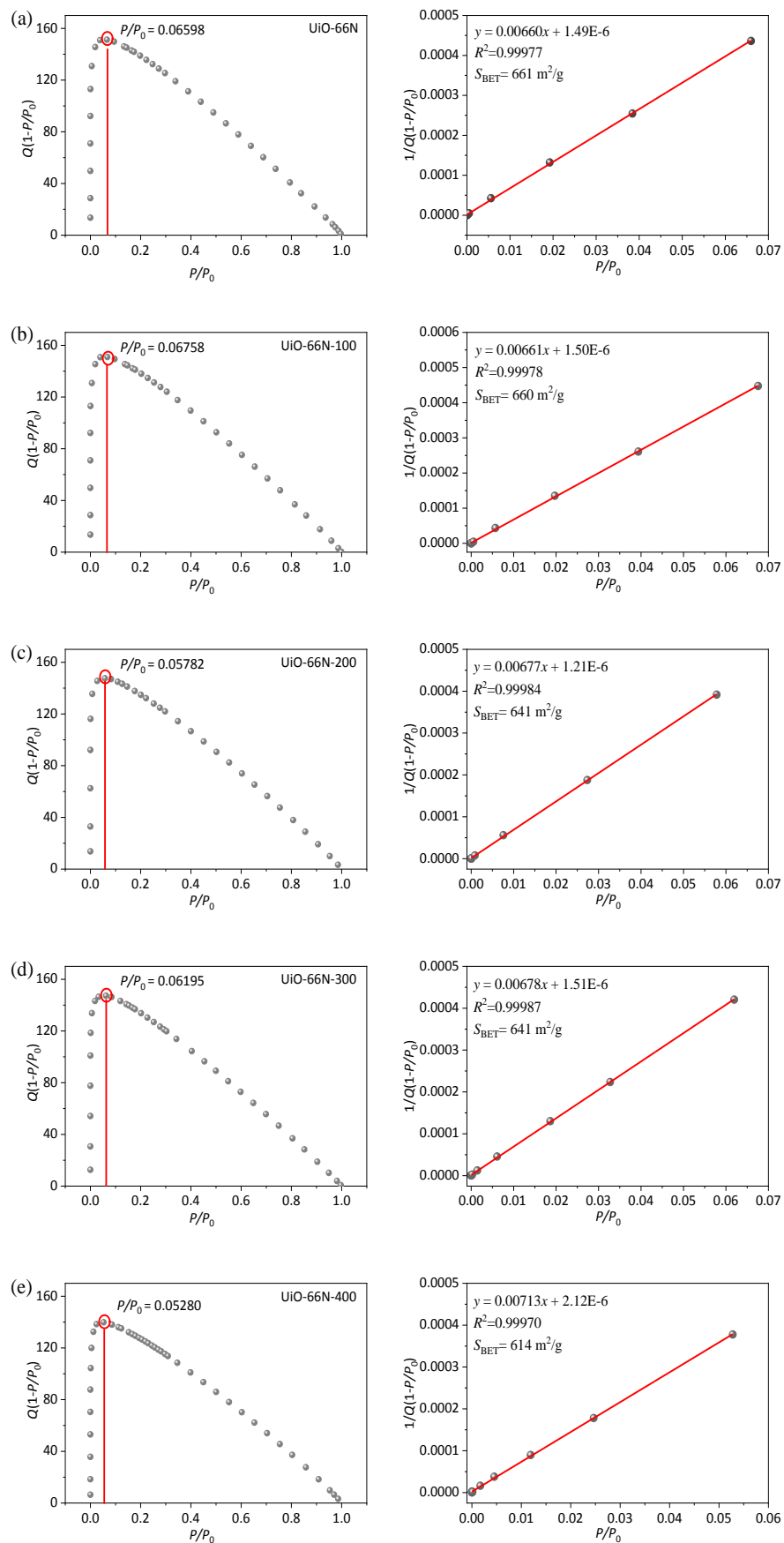


Figure S9. BET plots of (a) UiO-66N and (b-e) UiO-66N-X.

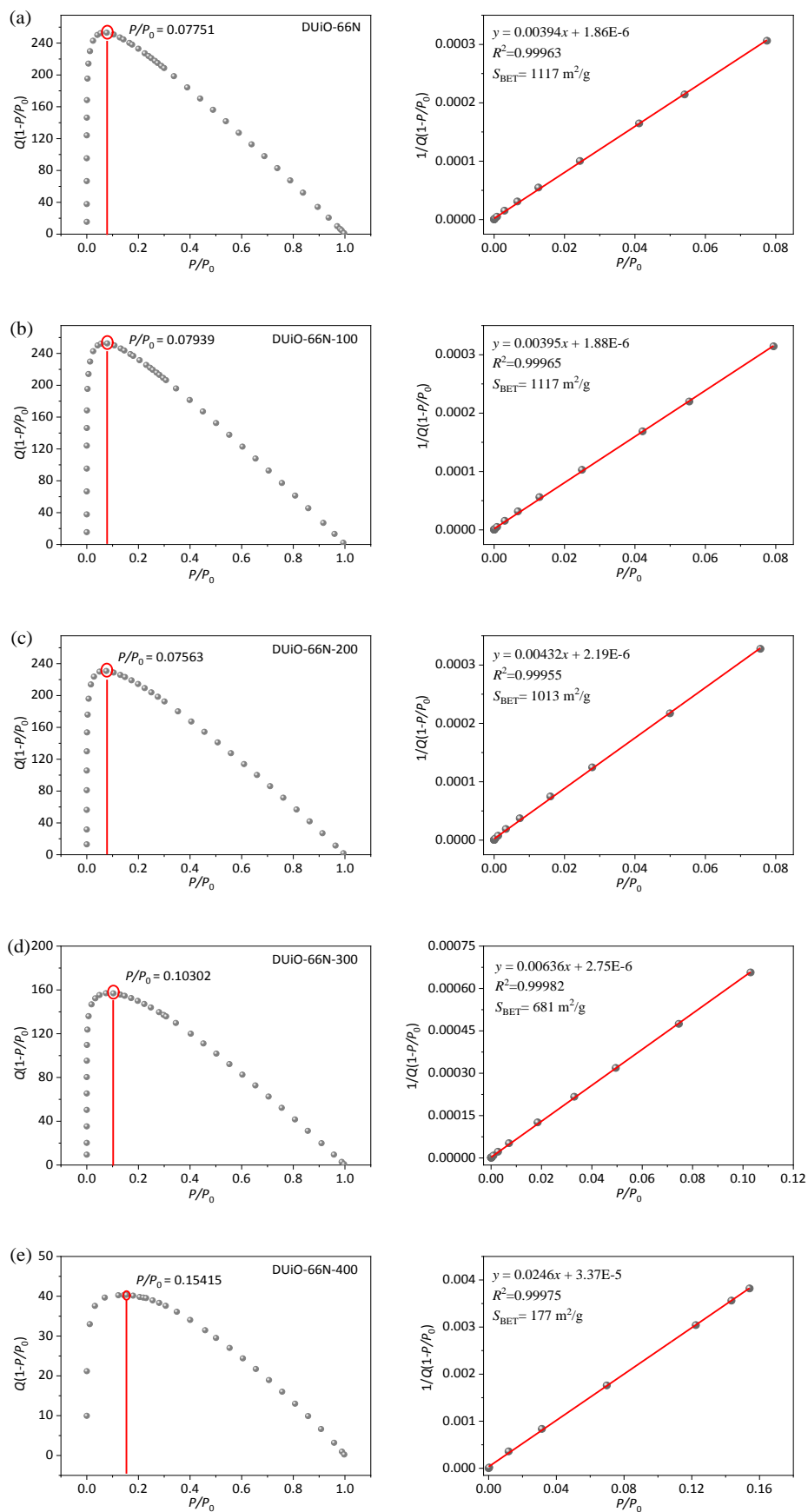


Figure S10. BET plots of (a) DUiO-66N and (b-e) DUiO-66N-X.

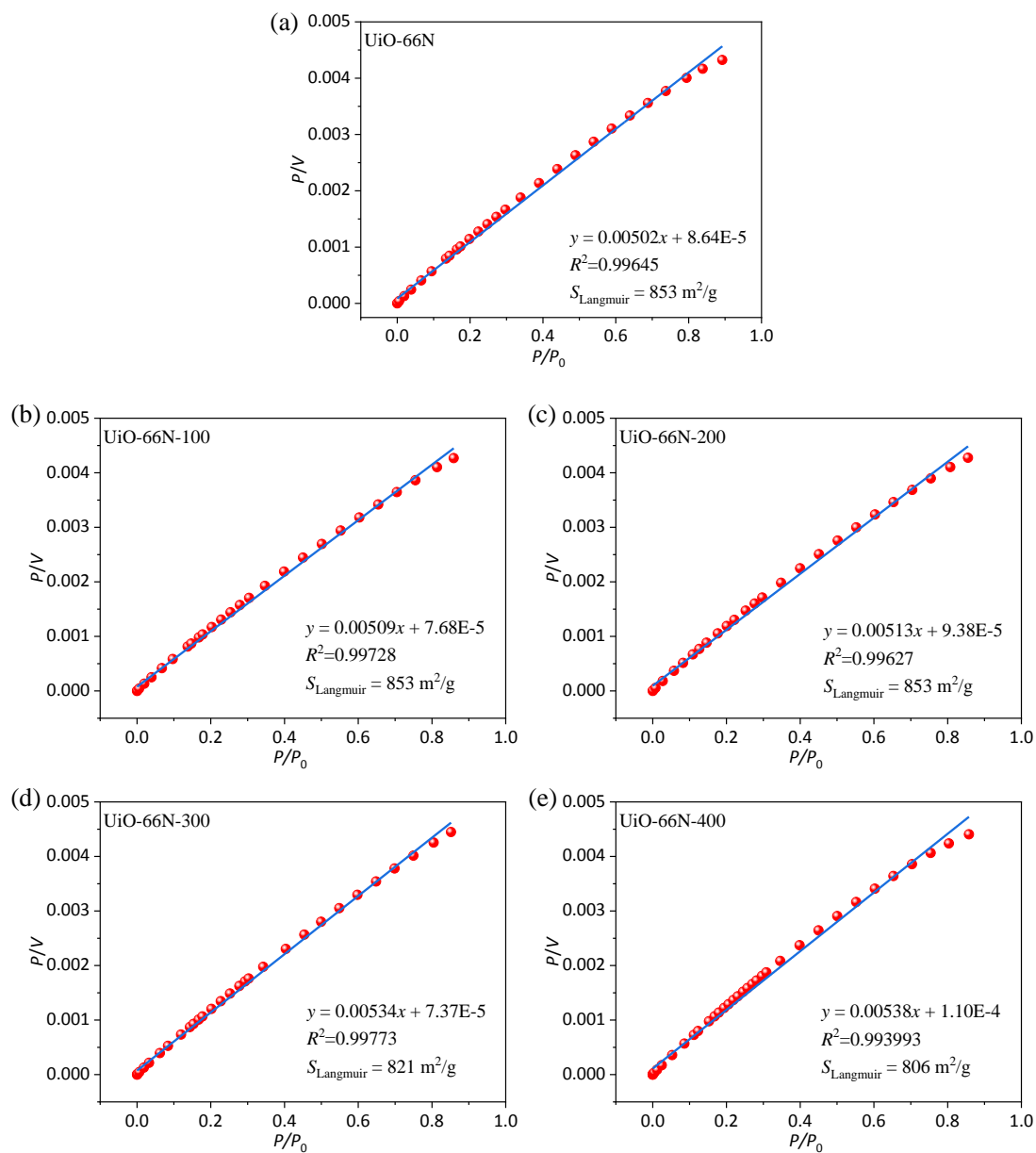


Figure S11. Langmuir plots of (a) UiO-66N and (b-e) UiO-66N-X.

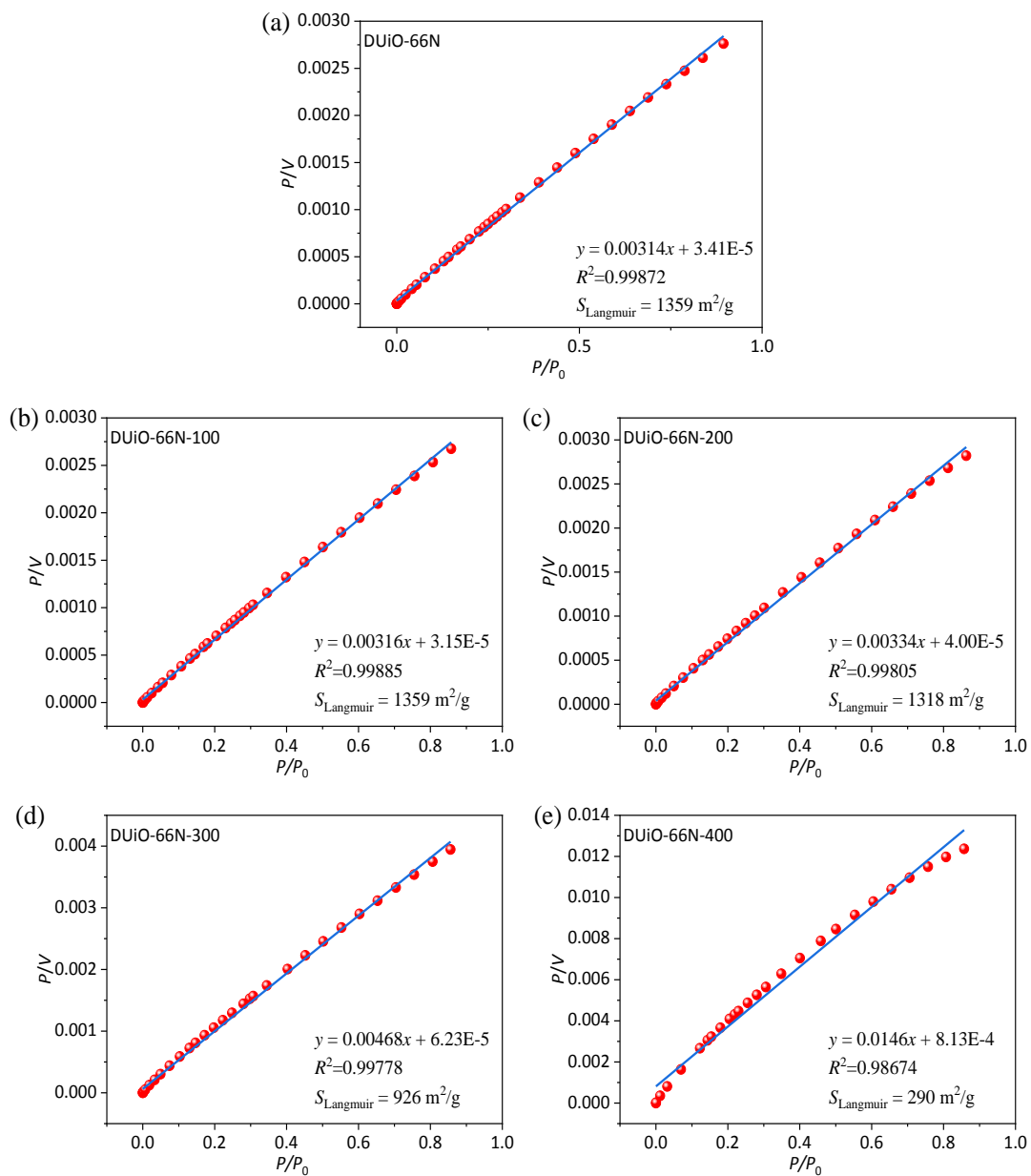


Figure S12. Langmuir plots of (a) DUiO-66N and (b-e) DUiO-66N-X.

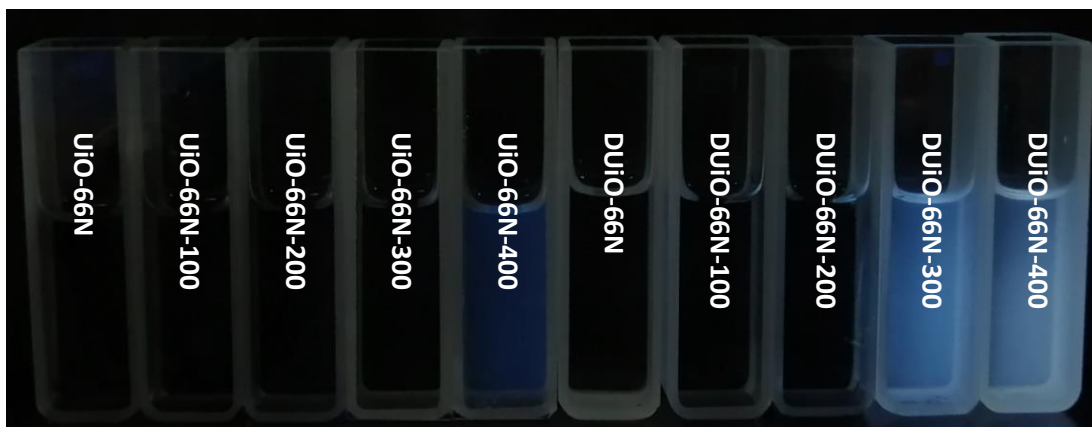


Figure S13. Photographs of the organic phase extract from digested samples under 365-nm UV light.

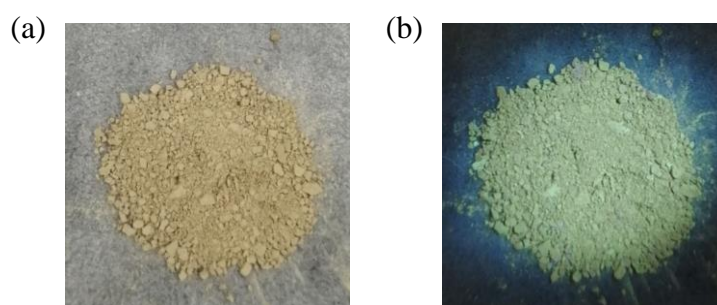


Figure S14. Photographs of CDs under (a) room light and (b) 365-nm UV light. Elemental analysis found(%): C : 85.72; H:12.22.

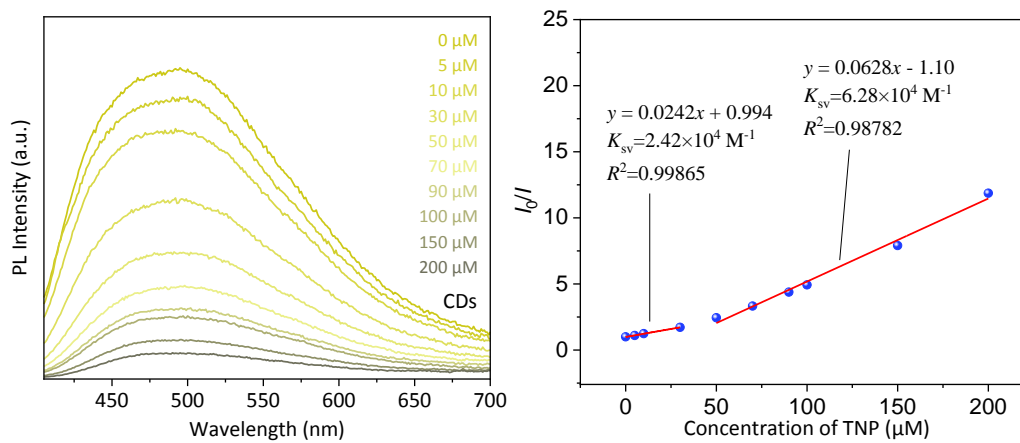


Figure S15. PL emission spectra in picric acid solutions with different concentrations ranging from 0 to 200 μM (left) and the Stern-Volmer fitting plots of CDs (right).

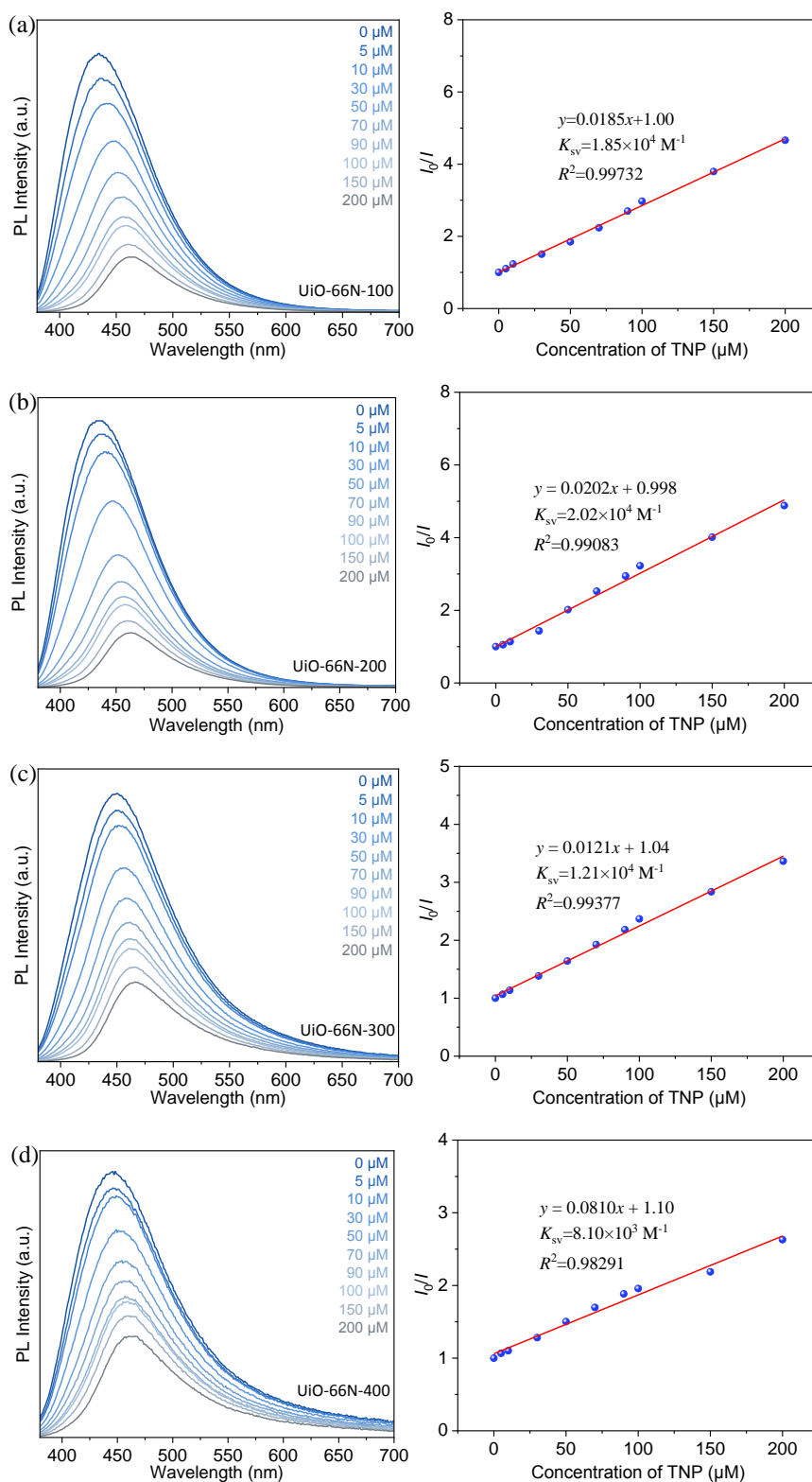


Figure S16. PL emission spectra in picric acid solutions with different concentrations ranging from 0 to 200 μM and Stern-Volmer fitting plots of (a) UiO-66N-100, (b) UiO-66N-200, (c) UiO-66N-300, and (d) UiO-66N-400.

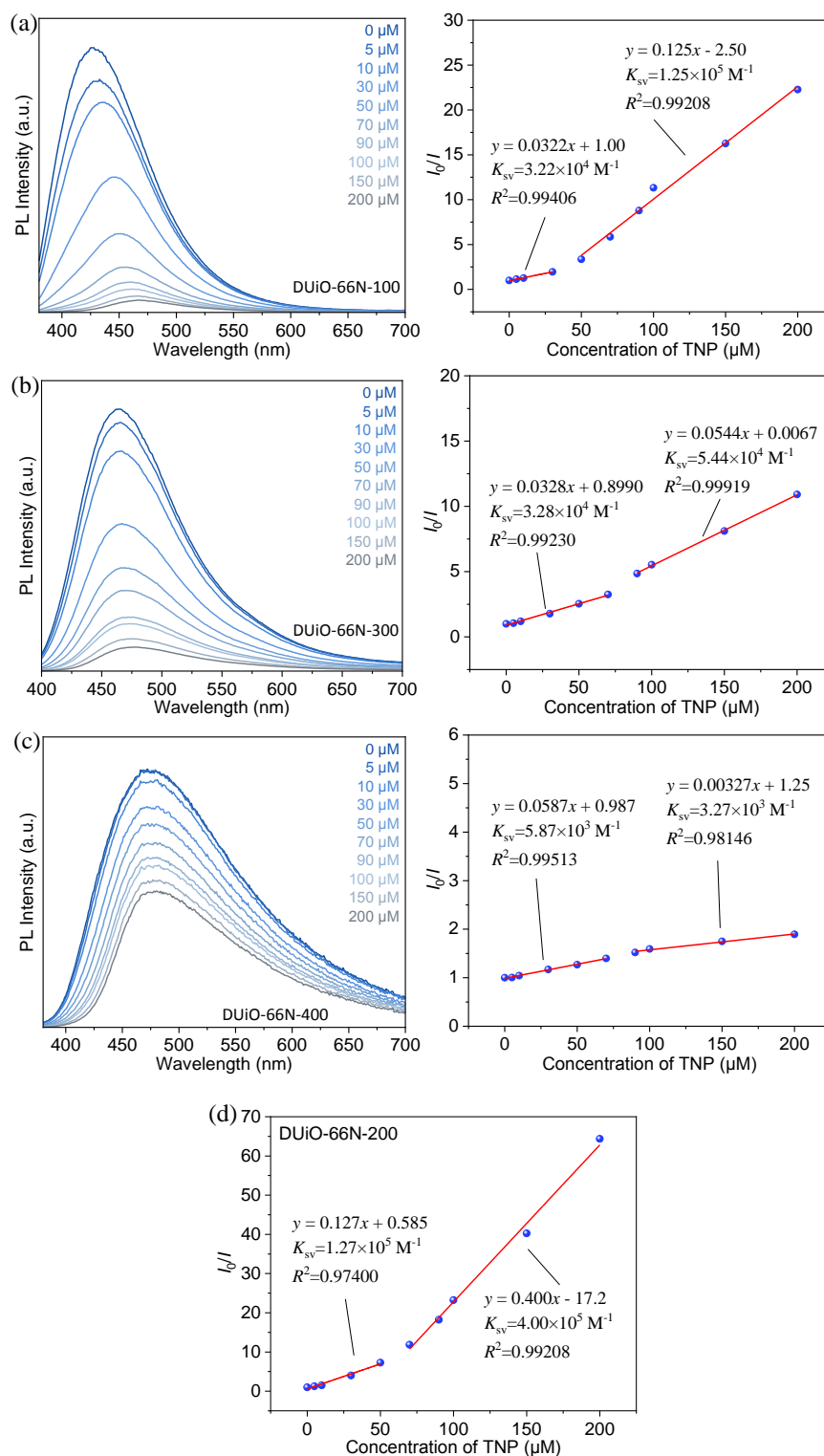


Figure S17. PL emission spectra in picric acid solutions with different concentrations ranging from 0 to 200 μM and Stern-Volmer fitting plots of (a) DUiO-66N-100, (b) DUiO-66N-300, and (c) DUiO-66N-400, and Stern-Volmer fitting plots of (d) DUiO-66N-200.

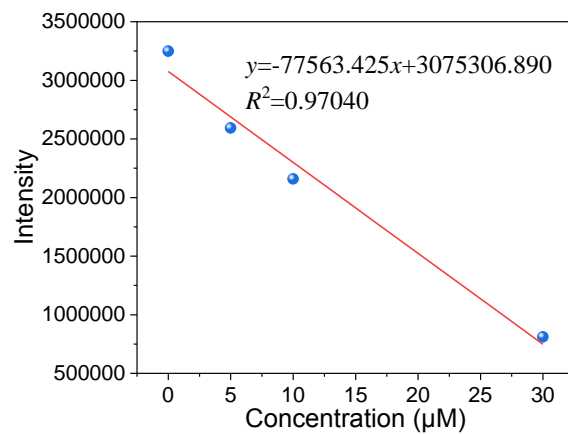


Figure S18. Intensity-concentration linear fitting of DUiO-66N-200 for the LOD evaluation.

Table S1. Structural model of UiO-66N for PXRD refinement.

UiO-66N				
Space group: <i>F23</i> (No.196)				
$a = b = c = 20.816(1) \text{ \AA}$				
$\alpha = \beta = \gamma = 90^\circ$				
$V = 9020(1) \text{ \AA}^3$				
Atom	<i>x</i>	<i>y</i>	<i>z</i>	Occupancy
Zr1	0.61545	0.50000	0.00000	1.0
O1	0.55812	0.55812	-0.05812	1.0
H1	0.58594	0.58594	-0.08594	1.0
O2	0.56024	0.56024	0.06024	1.0
O3	0.66873	0.49848	0.08898	1.0
O4	0.58893	0.4985	0.16878	1.0
C1	0.6496	0.49592	0.14966	1.0
C2	0.70084	0.48749	0.20091	1.0
C3	0.68392	0.48444	0.26763	1.0
H3	0.63313	0.48498	0.28269	0.5
C4	0.76755	0.48382	0.18392	1.0
H4	0.78254	0.48394	0.13311	0.5
C5	0.71536	0.49008	0.37852	0.5
H5	0.75212	0.49596	0.41871	0.5
C6	0.65313	0.48919	0.39214	0.5
H6	0.63895	0.48841	0.44505	0.5
C7	0.60902	0.48919	0.34804	0.5
H7	0.55611	0.48841	0.36221	0.5
C8	0.62265	0.49008	0.2858	0.5
H8	0.58241	0.49558	0.24903	0.5

Table S2. Porosity data of UiO-66N and DUiO-66N as well as their calcinated samples.

Sample	BET surface area (m ² /g)	Langmuir surface area (m ² /g)	pore volume (cm ³ /g, $P/P_0 = 0.2$)
UiO-66N	661	853	0.31
UiO-66N-100	660	853	0.30
UiO-66N-200	641	852	0.29
UiO-66N-300	641	821	0.28
UiO-66N-400	614	805	0.28
DUiO-66N	1117	1359	0.50
DUiO-66N-100	1117	1359	0.48
DUiO-66N-200	1013	1318	0.45
DUiO-66N-300	681	926	0.32
DUiO-66N-400	177	290	0.10

Table S3. Quenching data of UiO-66N-X and DUiO-66N-X.

sample \ Concentration of TNP (μM) I_0/I	0	5	10	30	50	70	90	100	150	200
UiO-66N-100	1.00	1.11	1.23	1.51	1.85	2.24	2.7	2.97	3.79	4.66
UiO-66N-200	1.00	1.05	1.14	1.43	2.02	2.53	2.94	3.22	4.01	4.88
UiO-66N-300	1.00	1.07	1.14	1.38	1.64	1.93	2.18	2.37	2.84	3.36
UiO-66N-400	1.00	1.07	1.10	1.28	1.50	1.70	1.88	1.96	2.19	2.63
DUiO-66N-100	1.00	1.15	1.26	1.96	3.36	5.85	8.79	11.33	16.26	22.27
DUiO-66N-200	1.00	1.25	1.51	4.00	7.26	11.87	18.24	23.21	40.23	64.34
DUiO-66N-300	1.00	1.05	1.19	1.78	2.53	3.25	4.86	5.53	8.11	10.91
DUiO-66N-400	1.00	1.00	1.04	1.17	1.27	1.40	1.52	1.59	1.75	1.89
CDs	1.00	1.10	1.24	1.72	2.45	3.33	4.38	4.93	7.90	11.87

Table S4. Comparison of luminescent sensing performance towards picric acid.

MOFs	Solvent	K_{sv} (M^{-1})	LOD	Ref.
DUiO-66N-200	MeOH	4.00×10^5	6.54×10^{-7} M	This work
$[Me_2NH_2]_4[Zn_6(qptc)_3(trz)_4] \cdot 6H_2O$	DMF	2.08×10^6	NA	[2]
Eu@MOF-253	EtOH	1.58×10^6	10 nM	[3]
$\{[Zn(adc)(avp)_2(H_2O)] \cdot (H_2O)_3\}_n$	MeCN	3.938×10^5	0.51×10^{-6} M	[4]
Cd@MOF	H ₂ O	2.176×10^5	0.54×10^{-6} M	[5]
$\{[Cd(\mu_2-BA)_2(ClO_4)_2] \cdot n(DCM)\}_n$	MeCN	1.39×10^5	0.054 μ M	[6]
$[Zn_4(DMF)(urotropine)_2(NDC)_4]$	H ₂ O	1.083×10^5	1.63 ppm (7.1 μ M)	[7]
$[Cd(L_2)] \cdot (DMF)_{0.92}$	DMF	9.3×10^4	0.3 ppm	[8]
$[Zn_2(NH_2BDC)_2(dpNDI)]_n$	H ₂ O	7.3×10^4	0.3 ppm (1.31 μ M)	[9]
$[Cd_5(TCA)_4(H_2O)_2]$	DMF	5.9×10^4	1.7 nM	[10]
$Zn_2(TZBPDC)(\mu_3-OH)(H_2O)_2$	CHCl ₃	4.9×10^4	2.78×10^{-7} M	[11]
$[Zn_3(bpg)_{1.5}(azdc)_3](DMF)_{5.9}(H_2O)_{1.05}$	DMF	4.6×10^4	0.4 μ M	[12]
$[Zn_2(TPOM)(NH_2-BDC)_2] \cdot 4H_2O$	DMF	4.60×10^4	9.8×10^{-7} M	[13]
$[Zn_8(ad)_4(BPDC)_6O \cdot 2Me_2NH_2] G$	H ₂ O	4.6×10^4	1.29×10^{-8} M	[14]
Zr-NDI MOF	H ₂ O	4.057×10^4	2.78×10^{-7} M	[15]
$Cd_4(L)_2(L_2)_3(H_2O)_2$	EtOH	3.89×10^4	1.98 ppm	[16]
$[(Zn_4O)(DCPB)_3] \cdot 11DMF \cdot 5H_2O$	DMF	3.7×10^4	NA	[17]
$[Cd_2(NDC)_{0.5}(PCA)_2] \cdot G_x$	MeCN	3.5×10^4	NA	[18]
$[Zn_2(Py_2TTz)_2(BDC)_2] \cdot 2(DMF) \cdot 0.5(H_2O)$	H ₂ O	3.257×10^4	0.93 μ M	[19]
$[(CH_3)_2NH_2]_3[Zn_4Na(L_3)_3] \cdot 4CH_3OH \cdot 2DMF$	DMF	3.2×10^4	0.1 mM	[20]
$\{[Zn_2(L)_2(azp)](DMF)_2 \cdot (H_2O)\}_n$	H ₂ O	3.11×10^4	0.00182 mM	[21]
$[\{Cu_2(L)(oba)_2\} \cdot DMF \cdot H_2O]_a$	MeOH	3.1×10^4	2.265×10^{-5} M	[22]
IRMOF-3	DMF/H ₂ O	2.99×10^4	0.1 ppm	[23]
$[Cu(L)(I)]_2 \cdot DMF \cdot MeCN$	MeCN	2.9×10^4	0.0066 mM	[24]
$Zr_6O_4(OH)_4(L)_6$	H ₂ O	2.9×10^4	2.6 μ M	[25]
UiO-68-mtpdc/etpdc	MeOH	2.8×10^4	NA	[26]
$[Zr_6O_4(OH)_4(BTDB)_6] \cdot 8H_2O \cdot 6DMF$	MeOH	2.49×10^4	1.63×10^{-6} M	[27]
$[Zn_2(L)_2(dpyb)]$	DMA	2.4×10^4	NA	[28]
$\{[Zn(IPA)(L)]\}_n$	H ₂ O	2.16×10^4	28 ppb	[29]
$[Eu_3(bpydb)_3(HCOO)(\mu_3-OH)_2(DMF)] \cdot (DMF)_3 \cdot (H_2O)_2$	H ₂ O	2.1×10^4	4.98 μ M	[30]
$[Tb_2(L_9)_3(H_2O)_2] \cdot 21H_2O$	H ₂ O	9.2×10^3	67 ppb	[31]

References

- [1] G. C. Shearer, S. Chavan, J. Ethiraj, J. G. Vitillo, S. Svelle, U. Olsbye, C. Lamberti, S. Bordiga, K. P. Lillerud, *Chem. Mater.* **2014**, *26*, 4068-4071.
- [2] X. X. Jia, R. X. Yao, F. Q. Zhang, X. M. Zhang, *Inorg. Chem.* **2017**, *56*, 2690-2696.
- [3] L. Chen, Z. Cheng, X. Peng, G. Qiu, L. Wang, *Anal. Methods* **2022**, *14*, 44-51.
- [4] S. Khan, A. Hazra, B. Dutta, Akhtaruzzaman, M. J. Raihan, P. Banerjee, M. H. Mir, *Cryst. Growth Des.* **2021**, *21*, 3344-3354.
- [5] A. Hazra, S. Bej, A. Mondal, N. C. Murmu, P. Banerjee, *ACS Omega* **2020**, *5*, 15949-15961.
- [6] S. I. Vasylevskiy, D. M. Bassani, K. M. Fromm, *Inorg. Chem.* **2019**, *58*, 5646-5653.
- [7] S. Mukherjee, A. V. Desai, B. Manna, A. I. Inamdar, S. K. Ghosh, *Cryst. Growth Des.* **2015**, *15*, 4627-4634.
- [8] S. Senthilkumar, R. Goswami, V. J. Smith, H. C. Bajaj, S. Neogi, *ACS Sustain. Chem. Eng.* **2018**, *6*, 10295-10306.
- [9] S. Singh Dhankhar, N. Sharma, S. Kumar, T. J. Dhilip Kumar, C. M. Nagaraja, *Chem. Eur. J.* **2017**, *23*, 16204-16212.
- [10] M. Venkateswarulu, A. Pramanik, R. R. Koner, *Dalton Trans.* **2015**, *44*, 6348-6352.
- [11] Y. Hu, M. Ding, X. Q. Liu, L. B. Sun, H. L. Jiang, *Chem. Commun.* **2016**, *52*, 5734-5737.
- [12] R. Goswami, S. C. Mandal, B. Pathak, S. Neogi, *ACS Appl. Mater. Interfaces* **2019**, *11*, 9042-9053.
- [13] R. Lv, J. Wang, Y. Zhang, H. Li, L. Yang, S. Liao, W. Gu, X. Liu, *J. Mater. Chem. A* **2016**, *4*, 15494-15500.
- [14] B. Joarder, A. V. Desai, P. Samanta, S. Mukherjee, S. K. Ghosh, *Chem. Eur. J.* **2015**, *21*, 965-969.
- [15] G. Radha, T. Leelasree, D. Muthukumar, R. S. Pillai, H. Aggarwal, *New J. Chem.* **2021**, *45*, 12931-12937.
- [16] T. K. Pal, N. Chatterjee, P. K. Bharadwaj, *Inorg. Chem.* **2016**, *55*, 1741-1747.
- [17] H. He, Y. Song, F. Sun, Z. Bian, L. Gao, G. Zhu, *J. Mater. Chem. A* **2015**, *3*, 16598-16603.
- [18] S. S. Nagarkar, B. Joarder, A. K. Chaudhari, S. Mukherjee, S. K. Ghosh, *Angew. Chem. Int. Ed.* **2013**, *52*, 2881-2885.
- [19] Z.-W. Zhai, S.-H. Yang, M. Cao, L.-K. Li, C.-X. Du, S.-Q. Zang, *Cryst. Growth Des.* **2018**, *18*, 7173-7182.
- [20] E.-L. Zhou, P. Huang, C. Qin, K.-Z. Shao, Z.-M. Su, *J. Mater. Chem. A* **2015**, *3*, 7224-7228.
- [21] S. Senthilkumar, R. Goswami, N. L. Obasi, S. Neogi, *ACS Sustain. Chem. Eng.* **2017**, *5*, 11307-11315.
- [22] P. Rani, Gauri, A. Husain, K. K. Bhasin, G. Kumar, *Cryst. Growth Des.* **2020**, *20*, 7141-7151.
- [23] J. Z. Wei, X. L. Wang, X. J. Sun, Y. Hou, X. Zhang, D. D. Yang, H. Dong, F. M. Zhang, *Inorg. Chem.* **2018**, *57*, 3818-3824.
- [24] S. Khatua, S. Goswami, S. Biswas, K. Tomar, H. S. Jena, S. Konar, *Chem. Mater.* **2015**, *27*, 5349-5360.
- [25] S. S. Nagarkar, A. V. Desai, S. K. Ghosh, *Chem. Commun.* **2014**, *50*, 8915-8918.
- [26] Q. Y. Li, Z. Ma, W. Q. Zhang, J. L. Xu, W. Wei, H. Lu, X. Zhao, X. J. Wang, *Chem. Commun.* **2016**, *52*, 11284-11287.
- [27] M. Sk, S. Biswas, *CrystEngComm* **2016**, *18*, 3104-3113.
- [28] Z. Q. Shi, Z. J. Guo, H. G. Zheng, *Chem. Commun.* **2015**, *51*, 8300-8303.
- [29] B. Parmar, Y. Rachuri, K. K. Bisht, R. Laiya, E. Suresh, *Inorg. Chem.* **2017**, *56*, 2627-2638.
- [30] X. Z. Song, S. Y. Song, S. N. Zhao, Z. M. Hao, M. Zhu, X. Meng, L. L. Wu, H. J. Zhang, *Adv. Funct. Mater.* **2014**, *24*, 4034-4041.
- [31] R. Fu, S. Hu, X. Wu, *J. Mater. Chem. A* **2017**, *5*, 1952-1956.